CrystEngComm

Accepted Manuscript

ROYAL SOCIETY OF CHEMISTRY

www.rsc.org/crystengcomm

Journal Name

RSCPublishing

ARTICLE

Anion-dependent assembly of Dy complexes: structures and magnetic behaviors

Cite this: DOI: 10.1039/x0xx00000x

Peng Chen,*[ab] Meiqi Zhang,[a] Wenbin Sun,[a] Hongfeng Li,[a] Lang Zhao[b] and Pengfei Yan*[a]

Received 00th January 2012,
Accepted 00th January 2012

DOI: 10.1039/x0xx00000x

www.rsc.org/

Self-assembly of 2-aldehyde-8-hydroxyquinoline, histamine dichloride and $LnX_3 \cdot 6H_2O$ (X^- = OAc^-, NO_3^- and ClO_4^-) affords a series of lanthanide complexes $Nd_3(nma)_2(OAc)_7 \cdot 3CH_3OH \cdot 0.5H_2O$ (**1a**), $Ln_3(nma)_2(OAc)_7 \cdot 2CH_3OH$ [Ln = Tb (**1b**) and Dy (**1c**)], $[Ln(nma)(NO_3)_2(DMSO)] \cdot CH_3OH$ [Ln = Nd (**2a**), Tb (**2b**), Dy (**2c**) and Er (**2d**)] and $[Dy(nma)_2] \cdot ClO_4 \cdot 0.5CH_3OH$ (**3**) (Hnma = N-(2-(8-hydroxylquinolinyl)methane(2-(4-imidazolyl)ethanamine)). It is noted that the formation and structures of **1**–**3** are anion-dependent, where diverse coordination modes are detected for acetates in trinuclear **1** as compared to single coordination mode for nitrates in mononuclear **2**. In the case of **3**, the Dy^{3+} ion is completely encapsulated by two ligands with uncoordinated perchlorate anion balancing the charge. Magnetic measurement shows that the Dy complexes of **1c**, **2c** and **3** exhibit slow relaxations under zero dc field. It is noted that single molecular magnet behavior is obtained for **2c** and **3** under an applied dc field of 2000 Oe.

Introduction

During the past decades, considerable attentions have been drawn on the designs, syntheses and characterization of lanthanide-containing compounds, which exhibit slow relaxation at the cryogenic temperature known as single molecular magnets (SMM).[1] The potential applications promote the research work of these magnetic materials,[2] and rich structures of SMMs have been prepared as mononuclear,[3] dinuclear,[4] trinuclear[5] and multinuclear complexes.[6] It is well believed that Dy^{3+} ions are the choice for the construction of SMMs, in respective to the high moment and anisotropy of the sip-orbit coupled Dy^{3+} Kramer ground state.[7] Accordingly, various ligands with multiple coordination sites have been employed to bind to the Dy^{3+} ions that it is widely accepted that the achievement of SMMs is governed by ligand field, coordination geometry and magnetic interactions between Ln^{3+} centers.[8] Recently, the *o*-vanillin-based Schiff-base ligands, as one of the most well-known species, have been focused on the preparation of SMMs with distinct anisotropic centers.[9] And the phenoxido-bridged compounds have consequently attracted considerable attentions, whilst rich SMMs have been reported to manipulate the coupling between lanthanide ions.[10]

8-hydroxyquinoline and its derivatives are important multidentate ligands, which could be utilized to bridge various metals and construct diverse compounds with intriguing properties.[11] In our previous studies, we have presented the successful encapsulation of Ln^{3+} ions through 2-aldehyde-8-hydroxyquinoline-based (ahq) ligand.[12] In order to get controllable coordination geometry of the lanthanide complexes, we prefer to extend the coordination ability of ahq by attaching histamine moiety, giving rise to the formation of the ligand N-(2-(8-hydroxylquinolinyl)methane(2-(4-imidazolyl)ethanamine) (Hnma), which is utilized to coordinate to Ln^{3+} ions in pursuit of complexes with intriguing magnetic behavior.

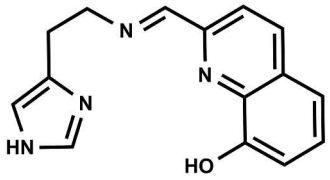

Scheme 1. The molecular structure of the ligand Hnma.

Meanwhile, great efforts have been devoted to the crystal engineering for the fabrication of functional materials, on account of the significant contribution of the structures and compositions to the potential properties.[13] The synthesis is often complicated due to the versatile coordination geometries of the lanthanide ions, and the structural diversity is accompanied with a variety of factors such as ionic radius, the nature of the counter ions, the structure of the ligand and so on.[14] The importance of the anions in the self-assembly is less noted, although they can tune the structures through their diversified coordination modes.[15] Recent example has demonstrated the importance of Cl^- anions in the self-assembly of 24-metal and 32-metal complex that offers an opportunity to study the formation of high-nuclearity clusters in NIR property.[16] We herein present the syntheses, structures and characterization of a series of lanthanide complexes $[Nd_3(nma)_2(OAc)_7] \cdot 3CH_3OH \cdot 0.5H_2O$ (**1a**), $[Ln_3(nma)_2(OAc)_7] \cdot 2CH_3OH$ [Ln = Tb (**1b**) and Dy (**1c**)], $[Ln(nma)(NO_3)_2(DMSO)] \cdot CH_3OH$ [Ln = Nd (**2a**), Tb (**2b**), Dy (**2c**) and Er (**2d**)] and $[Dy(nma)_2] \cdot ClO_4 \cdot 0.5CH_3OH$ (**3**), which

are obtained from the in-situ condensation of $LnX_3{\cdot}6H_2O$ (X= OAc^-, NO_3^-, ClO_4^-), ahq and histamine. The result highlights significant role of the anions with distinct coordination modes in the assembly of **1**−**3** that three distinct species complexes have been prepared under the similar condition. Magnetic measurement shows that **1c**, **2c** and **3** exhibit slow relaxations of the magnetization.

Experimental section

Materials and Measurements

The commercially available chemicals were analytical reagent grade and used without further purification. 2-Aldehyde-8-hydroxyquinoline (ahq) was synthesized according to the reported methods.[17] The ligand N-(2-(8-hydroxylquinolinyl)methane(2-(4-imidazolyl)ethanamine) (Hnma) was in-situ formed by the condensation of ahq and histamine in the reaction system (Scheme 1). Elemental analyses were performed on an Elementar Vario EL cube analyzer. FT-IR spectra were obtained on a Perkin-Elmer Spectrum One spectrophotometer by using KBr disks in the range of 4000–370 cm^{-1}. The magnetic susceptibility measurements were obtained using a Quantum Design SQUID magnetometer MPMS-3 operating between 2 and 300 K for dc-applied fields ranging from −7 to 7 T, ac susceptibility measurements were carried out under an oscillating ac field of 2 Oe and ac frequencies ranging from 1 to 1000 Hz. A diamagnetic correction was applied for the sample holder. X-ray powder diffraction data were collected on a Bruker D5005 X-ray diffractometer with Cu *Kα* radiation (λ = 1.5406 Å). Thermogravimetric analyses were obtained on an SDT Q600 thermogravimetric analyzer at a heating rate of 20 °C/min under air atmosphere in the temperature range of 25–780 °C. All measurements were carried out by using fresh crystals.

Single crystals of **1**−**3** were selected for X-ray diffraction analysis on a Xcalibur, Eos diffractometer using graphite-monochromated Mo-K*α* radiation (λ = 0.71073 Å). The crystals were kept under N_2 atmosphere at 150K for **1** and 293K for **2** and **3** during data collection. The structures were solved by the direct methods and refined on F^2 by full-matrix least-square using the SHELXTL-97 program.[18] The Ln^{3+} ions were firstly located, and then non-hydrogen atoms (C, N, O, S and Cl) were placed from the subsequent Fourier-difference maps and refined anisotropically. The H atoms were introduced in the calculated positions and refined with fixed geometry with respect to their carrier atoms. Large residual Fourier peaks and holes near the metal ions in **1a**−**1c** were detected, which would be probably owing to the accounted twinning. The absorption correction had been tried times, but it had not improved. In **1a**−**1c**, the diffused electron densities resulting from the residual solvents were removed from the dataset by using the SQUEEZE routine of PLATON and it was further refined using the data generated.[19] With respects to the TG analyses and the solvents added, it was supposed two more (**1a**) and eight (**1b** and **1c**) methanol molecules were included, respectively, which had been added in the unit cell contents. The crystallographic formulae (**1a**−**1c**) have been modified to include non-located atoms. More details concerned with constraints and the refinements had been supplied in the cif files. The experimental details for the structural determination are presented in Table 1.

Synthesis of 1−3

$[Nd_3(nma)_2(OAc)_7]{\cdot}3CH_3OH{\cdot}0.5H_2O$ (1a)

Self-assembly reactions of ahq, histamine dihydrochloride, triethylamine and $Ln(OAc)_3{\cdot}6H_2O$ [Ln= Nd (**1a**), Tb (**1b**), Dy (**1c**)] afforded the corresponding complexes **1a**−**1c**, respectively (Scheme 2). For the case of **1a**: 0.129 g (0.3 mmol) $Nd(OAc)_3{\cdot}6H_2O$, 0.017 g (0.1 mmol) ahq, 0.018 g (0.1 mmol) histamine dihydrochloride and 0.010 g (0.1 mmol) triethylamine were dissolved in a mixture of CH_3OH/CH_2Cl_2 (5/10 ml, v/v). Then diethyl ether was allowed to diffuse slowly into the filtrate. Crystals of **1a** suitable for single crystal X-ray analysis could be obtained in 9 days. Anal. Calcd for $C_{47}H_{60}N_8Nd_3O_{19.5}$ (1481.75): C, 38.10; H, 4.01; N, 7.56 wt%. Found: C, 38.14; H, 4.03; N, 7.59 wt%. IR (KBr, cm^{-1}): 3386, 3158, 2915, 1547, 1449, 1104, 1016, 843, 765, 670.

$[Tb_3(nma)_2(OAc)_7]{\cdot}2CH_3OH$ (1b)

Anal. Calcd for $C_{46}H_{55}N_8O_{18}Tb_3$ (1484.72): C, 37.21; H, 3.73; N, 7.55 wt%. Found: C, 37.29; H, 3.85; N, 7.50 wt%. IR (KBr, cm^{-1}): 3380, 3103, 2920, 1556, 1456, 1106, 1019, 845, 766, 672.

Table 1 Crystal data and structural refinement parameters for **1**–**3**.

Identification	1a	1b	1c	2a	2b	2c	2d	3
Empirical formula	$C_{47}H_{60}N_8Nd_3O_{19.5}$	$C_{46}H_{55}N_8O_{18}Tb_3$	$C_{46}H_{55}Dy_3N_8O_{18}$	$C_{18}H_{23}N_6NdO_9S$	$C_{18}H_{23}N_6O_9STb$	$C_{18}H_{23}DyN_6O_9S$	$C_{18}H_{23}ErN_6O_9S$	$C_{30.5}H_{28}ClDyN_8O_{6.5}$
Formula weight	1481.75	1484.74	1495.48	643.72	658.40	661.98	666.75	808.56
Cryst. syst.	triclinic	triclinic	triclinic	triclinic	triclinic	triclinic	triclinic	monoclinic
Space group	$P\bar{1}$	$P\bar{1}$	$P\bar{1}$	$P\bar{1}$	$P\bar{1}$	$P\bar{1}$	$P\bar{1}$	$P2_1/c$
a (Å)	17.0393(6)	16.8042(7)	16.7829(7)	9.4831(4)	9.4373(5)	9.421(2)	9.3532(7)	18.1140(3)
b (Å)	17.8176(6)	17.6752(6)	17.6513(6)	10.3029(4)	10.2862(6)	10.2707(17)	10.1772(4)	15.7015(2)
c (Å)	20.2468(7)	19.4071(11)	19.3643(11)	12.9928(5)	12.9039(6)	12.909(2)	12.8201(5)	22.3234(3)
α (°)	112.788(3)	69.390(4)	69.388(4)	86.142(3)	85.730(4)	85.595(14)	85.678(3)	90
β (°)	97.045(3)	82.993(4)	83.013(4)	87.700(3)	88.061(4)	87.715(16)	87.922(4)	97.683(2)
γ (°)	90.308(3)	89.895(3)	89.894(3)	76.628(3)	76.723(5)	76.894(16)	76.710(5)	90
Volume ($Å^3$)	5614.9(3)	5349.8(4)	5324.2(4)	1231.83(9)	1215.59(11)	1212.6(4)	1184.05(11)	6292.16(16)
Z	4	4	4	2	2	2	2	8
R_{int}	0.0559	0.0968	0.0907	0.0328	0.0288	0.0783	0.0255	0.0373
GOF of F^2	1.028	1.089	0.990	1.065	1.037	1.043	1.055	1.013
Final *R* [$I>2\sigma(I)$] indices	R_1 = 0.0875	R_1 = 0.0884	R_1 = 0.0772	R_1 = 0.0238	R_1 = 0.0281	R_1 = 0.0350	R_1 = 0.0239	R_1 = 0.0370
	wR_2 = 0.2228	wR_2 = 0.2148	wR_2 = 0.1950	wR_2 = 0.0523	wR_2 = 0.0538	wR_2 = 0.0868	wR_2 = 0.0541	wR_2 = 0.0744
R indices (all data)	R_1 = 0.1129	R_1 = 0.1396	R_1 = 0.1218	R_1 = 0.0286	R_1 = 0.0345	R_1 = 0.0386	R_1 = 0.0265	R_1 = 0.0553
	wR_2 = 0.2401	wR_2 = 0.2518	wR_2 = 0.2272	wR_2 = 0.0550	wR_2 = 0.0569	wR_2 = 0.0901	wR_2 = 0.0556	wR_2 = 0.0826

$[Dy_3(nma)_2(OAc)_7]\cdot 2CH_3OH$ (1c)

Anal. Calcd for $C_{46}H_{55}Dy_3N_8O_{18}$ (1495.48): C, 36.94; H, 3.71; N, 7.49 wt%. Found: C, 37.02; H, 3.81; N, 7.43 wt%. IR (KBr, cm^{-1}): 3394, 3114, 2925, 1558, 1456, 1107, 1018, 837, 767, 673.

$[Nd(nma)(NO_3)_2(DMSO)]\cdot CH_3OH$ (2a)

2a-2d were prepared as above starting from $Ln(NO_3)_3\cdot 6H_2O$ [Ln = Nd (**2a**), Tb (**2b**), Dy (**2c**) and Er (**2d**)]. For the case of **2a**, $Nd(NO_3)_3\cdot 6H_2O$ 0.088 g (0.2 mmol), 0.034 g (0.2 mmol) ahq, 0.036 g (0.2 mmol) histamine dihydrochloride and 0.020 g (0.2 mmol) triethylamine were dissolved in a mixture of CH_3OH/CH_2Cl_2/DMSO (2/5/1 ml, v/v/v). Then diethyl ether was allowed to diffuse slowly into the filtrate. Crystals suitable for single crystal X-ray analysis could be obtained in 7 days. Anal. Calcd for $C_{18}H_{23}N_6NdO_9S$ (643.72): C, 33.59; H, 3.60; N, 13.06; S, 4.98 wt%. Found: C, 33.59; H, 3.61; N, 13.06; S, 4.98 wt%. IR (KBr, cm^{-1}): 3316, 3142, 3019, 2909, 1636, 1593, 1457, 1385, 1285, 1105, 1006, 843, 735.

$[Tb(nma)(NO_3)_2(DMSO)]\cdot CH_3OH$ (2b)

Anal. Calcd for $C_{18}H_{23}N_6O_9STb$ (658.40): C, 32.84; H, 3.52; N, 12.76; S, 4.87 wt%. Found: C, 32.83; H, 3.54; N, 12.78; S, 4.88 wt%. IR (KBr, cm^{-1}): 3314, 3151, 3023, 2909, 1637, 1595, 1459, 1384, 1304, 1106, 1009, 843, 741.

$[Dy(nma)(NO_3)_2(DMSO)]\cdot CH_3OH$ (2c)

Anal. Calcd for $C_{18}H_{23}N_6DyO_9S$ (661.98): C, 32.66; H, 3.50; N, 12.70; S, 4.84 wt%. Found: C, 32.68; H, 3.49; N, 12.70; S, 4.85 wt%. IR (KBr, cm^{-1}): 3311, 3140，3024, 2914, 1637, 1598, 1459, 1381, 1308, 1108, 846, 738.

$[Er(nma)(NO_3)_2(DMSO)]\cdot CH_3OH$ (2d)

Anal. Calcd for $C_{18}H_{23}N_6ErO_9S$ (666.75): C, 32.43; H, 3.48; N, 12.60; S, 4.81 wt%. Found: C, 32.45; H, 3.49; N, 12.60; S, 4.79 wt%. IR (KBr, cm^{-1}): 3311, 3113, 3026, 2912, 1639, 1596, 1461, 1384, 1306, 1106, 1008, 842, 743.

$[Dy(nma)_2]\cdot ClO_4\cdot 0.5CH_3OH$ (3)

0.057 g (0.1 mmol) $Dy(ClO_4)_3\cdot 6H_2O$, 0.034 g (0.2 mmol) ahq, 0.036 g (0.2 mmol) histamine dihydrochloride and 0.020 g (0.2 mmol) triethylamine were dissolved in CH_3OH solution (5 ml). Then diethyl ether was allowed to diffuse slowly into the filtrate. Crystals suitable for single crystal X-ray analysis could be obtained in 6 days. Anal. Calcd for $C_{30.5}H_{28}ClDyN_8O_{6.5}$ (808.56): C, 45.31; H, 3.49; N, 13.86 wt%. Found: C, 45.29; H, 3.48; N, 13.84 wt%. IR (KBr, cm^{-1}): 3395, 3011, 2921, 1631, 1591, 1457, 1337, 1106, 838, 764, 622.

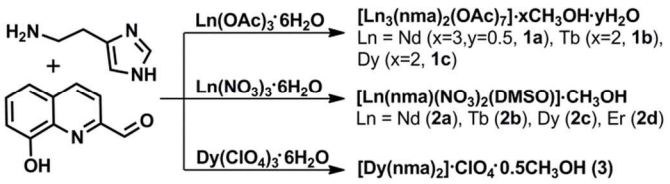

Scheme 2. The synthetic routes of **1**−**3**.

Results and Discussion

Structural description of 1–3

Single crystal X-ray diffraction analysis reveals that **1a**–**1c** are isostructural and crystallize in the triclinic space group $P\bar{1}$. Therefore, a full description of **1c** is given as a representative example. In the asymmetric unit of **1c**, there are two crystallographically independent $[Dy_3(nma)_2(OAc)_7]$ units, which adopt nearly linear arrangements (Figure 1). Dy1, Dy2 and Dy3 ions possess the similar coordination environments to Dy4, Dy5 and Dy6 ions, respectively, so the moiety containing Dy1 ion are selected to describe the structural feature. Dy1 ion is nine-coordinated to one O and three N atoms of the ligand and five O atoms from the acetate groups. Dy2 ion is nine-connected to seven O atoms from the acetate groups, and two O atoms of the ligand. Dy3 ion is nine-ligated to one O and three N atoms of the ligand, and five O atoms from the acetate groups as well. The Dy–O(N) bond lengths are in the range of 2.288(13)–2.570(10) Å in accordance with the reported values. The N_{imino} atoms are exclusively kept connected to the Dy ions, while the N_{amino} atoms remain uncoordinated in contrast. The Dy1···Dy2 and Dy2···Dy3 distances of 3.6700(7) and 3.7991(8) Å are similar to that of Dy4···Dy5 and Dy5···Dy6 (3.6539(8) and 3.8562(8) Å), which are compatible to those in the Ln_3 triangles.[7b,7c,20] Various coordination modes have been detected for acetate groups in **1c**, which act as a bridge between the terminal and central Dy^{3+} ions in addition to the phenoxido bridges.[21] Dy1 and Dy2 ions share two acetate groups in the chelating-bridging mode, and Dy2 and Dy3 ions share as well two acetate groups in the chelating-bridging and bridging modes, respectively. The intermolecular N–H···O H-bonds are found among the two crystallographically distinct units, while π-π interactions could be observed among the quinolinyl groups (Figure 2). It is noted that only chelating and chelating bridging coordination modes are detected in **1a**, although the Nd···Nd distances are in the similar range of 3.7855(8)–3.8331(8) Å.

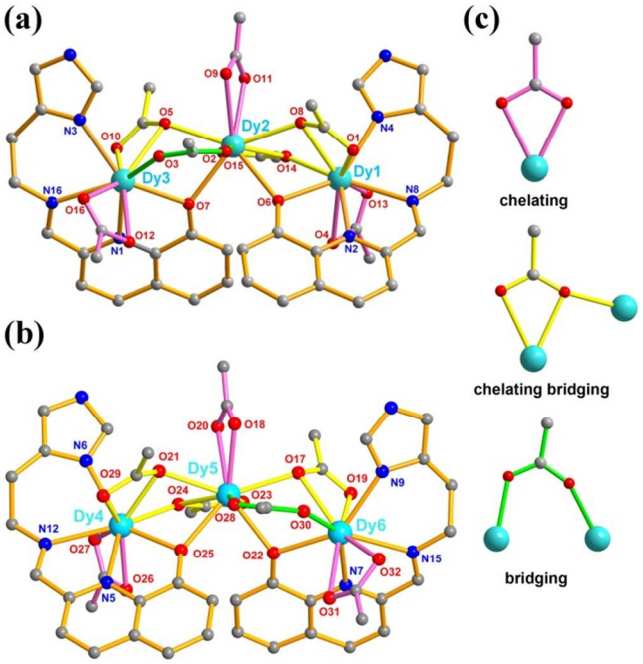

Figure 1. Partially labeled units containing Dy1 (a) and Dy4 ions (b) in **1c** (Hydrogen atoms have been omitted for clarity); (c) three coordination modes found for acetates in **1c**.

X-ray crystallographic analysis reveals that **2a**–**2d** are isomorphous and crystallize in the triclinic space group $P\bar{1}$, and the structure of **2c** is described as an example. In the asymmetric unit of **2c**, there are one Dy ion, one ligand, two nitrate groups, one methanol and one DMSO molecules (Figure 3). Dy1 ion is nine-coordinated to three N atoms and six O

atoms in a muffin arrangement.[22] Referring to the ligand, the two crystallographically distinct nitrate groups axially chelate Dy1 ion and the DMSO molecule is horizontally attached to the Dy1 ion. The Dy−O(N) distances are in the range of 2.314(3)−2.563(3) Å, whilst the distances of Dy−O (phenolate and sulfoxide O atoms) are significantly shorter. The π−π interactions could be detected with the overlap of the quinolinyl groups of the adjacent [Dy(nma)$(NO_3)_2$(DMSO)] units. And intermolecular H-bonds are found among the unit and methanol molecule with N(O)···O 2.772(5) Å and 2.683(4) Å, respectively.

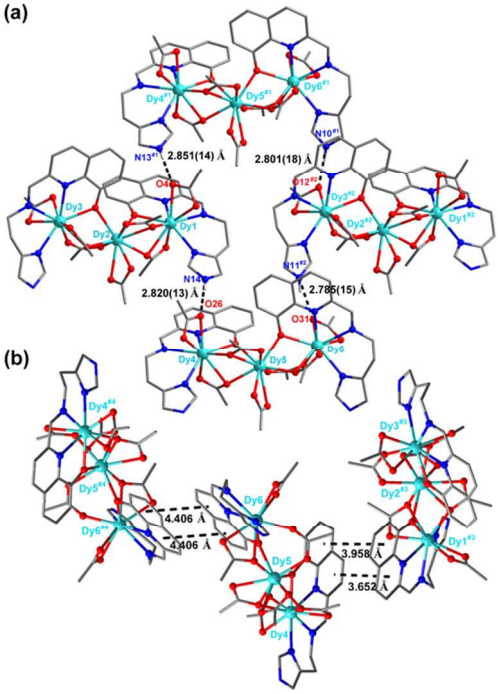

Figure 2. Views showing the intermolecular H-bonding (a) and π-π interactions (b) in **1c**. (Hydrogen atoms have been omitted for clarity; symmetry codes: #1: x, y-1, z; #2: x+1, y, z; #3: 2-x, 2-y, -z; #4: 1-x, 1-y, 1-z)

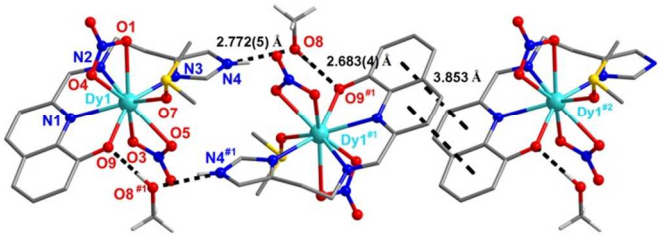

Figure 3. Partially labeled crystal structure and a view showing the intermolecular H-bonding and π-π interactions in **2c**. (Hydrogen atoms have been omitted for clarity; symmetry codes: #1:2-x, -y, -z; #2: x, y-1, z-1)

X-ray crystallographic analysis reveals that **3** crystallizes in the monoclinic space group $P2_1/c$. In the asymmetric unit of **3**, there are two crystallographically distinct $[Dy(nma)_2]^+$ units, one methanol molecule and two perchlorate groups (Figure 4). Each Dy^{3+} ion encapsulated by two ligands is eight-coordinated to two O atoms and six N atoms, adopting a biaugmented trigonal prism arrangement. The Dy−O distances are in the range of 2.260(3)−2.300(3) Å and Dy−N distances are in the range of 2.464(4)−2.631(4) Å. The π−π interactions could be detected with the overlap of the quinolinyl groups of the two adjacent crystallographically equivalent $[Dy1(nma)_2]^+$ units, while the π−π interactions between two adjacent crystallographically equivalent $[Dy(nma)_2]^+$ units is arisen from the overlap of imidazolyl and quinolinyl groups. Furthermore, the two crystallographically distinct units form π−π interactions as well. The intermolecular H-bonds with N−H···O distances of 2.703(5) and 2.773(5) Å are observed among the crystallographically equivalent units, whilst H-bonds with N−H···O distances of 2.935(5) and 3.023(6) Å among the perchlorate and imidazolyl groups.

Similar results could be obtained with equivalent NaOH instead of triethylamine for **1**–**3**, while all attempts to synthesize complexes incorporated with chlorides were unsuccessful. Initially, the attempt for **2** were prepared by using a solution of CH_3OH/CH_2Cl_2, where precipitates formed and only small crystals were found in very low yield. We therefore adjust the synthetic condition to improve the solubility through the addition of a few DMSO into the reaction mixture. As expected, the reaction solution tuned to clear and large crystals in high yield were collected. The stoichiometry and structures of these complexes are dependent on the nature of the anion, and the presence of different anions OAc^-, NO_3^- and ClO_4^- provided by the lanthanide salts has made significant contribution to the formation of diversified structures of **1**–**3**. The successful preparation of trinuclear **1** is attributed to the variable coordination modes of the acetate anions to the lanthanide ions, while nitrate groups are bound to the Ln^{3+} ions in the chelating mode as a terminal in **2**. And mononuclear **3** encapsulated by two ligands is obtained by the introduction of uncoordinated perchlorate. The anions in versatile coordination modes would facilitate the formation of multinuclear complexes.

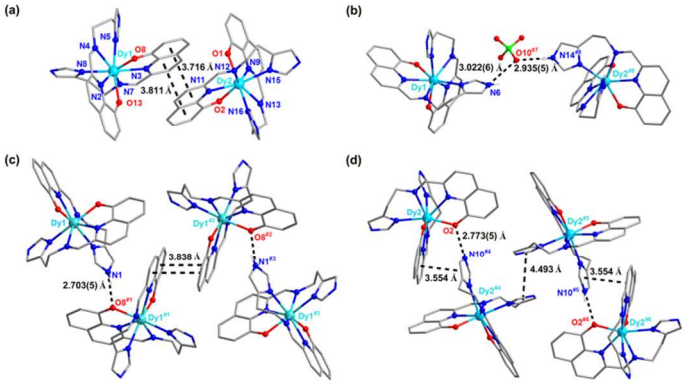

Figure 4. Partially labeled crystal structure of **3** and the π-π interactions (a), and intermolecular H-bonding among Dy1 and Dy2 units (b). Views showing the intermolecular H-bonding and π-π interactions among the crystallographically equivalent Dy1 units (c) and Dy2 units (d), respectively. (Hydrogen atoms have been omitted for clarity; symmetry codes: #1: 1-x, -0.5+y, 0.5-z; #2: x, 1.5-y, 0.5+z; #3: 1-x, 1-y, 1-z; #4: -x, -0.5+y, 0.5-z; #5: x, 1.5-y, z-0.5; #6: -x, 1-y, -0.5+z; #7: 1-x, 0.5+y, 0.5-z; #8: 1+x, 1.5-y, -0.5+z)

Magnetic properties of 1c, 2c and 3

The direct-current (dc) magnetic measurements are performed in an applied magnetic field of 1000 Oe (Figure 5) for **1c**, **2c** and **3** in the temperature range of 2–300 K. At the

room temperature, the values of χT are 82.94, 14.09 and 14.14 cm^3 K mol^{-1} for complexes **1c**, **2c** and **3**, respectively, which are close to the expected value for six, one and two independent Dy^{3+} ions (**1c**: 85.02, **2c**: 14.17, **3**: 14.17 cm^3 K mol^{-1}): Dy^{3+} (S = 5/2, L = 5, $^6H_{15/2}$, g = 4/3, C =14.17 cm^3 K mol^{-1}). For **1c**, the χT product remained constant down to 75 K on lowering the temperature before dropping rapidly down to 40.96 cm^3 K mol^{-1} at 2 K. The decrease of χT at low temperature obviously suggests the presence of intramolecular antiferromagnetic interactions within Dy^{3+} ions. Similar results can be observed for complexes **2c** and **3**. The χT products gradually decrease on lowering the temperature and drop to minimum values of 9.98 and 11.62 cm^3 K mol^{-1} at 2 K. The gradual decrease before 75 K is due to the thermal depopulation of the Stark sublevels, whereas the latter rapid drop may be ascribed to the weak antiferromagnetic interactions between the lanthanide centers, even if magnetic anisotropy might also partially affect low temperature susceptibility.

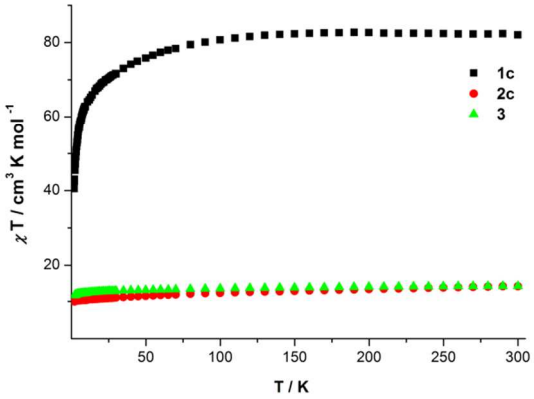

Figure 5. Temperature dependence of the χT products at 1000 Oe.

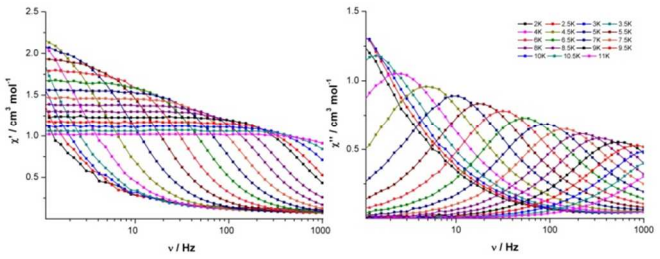

Figure 6. The frequency dependence of the out-of-phase ac susceptibility of **2c** at the indicated temperature under an applied dc field of 2000 Oe.

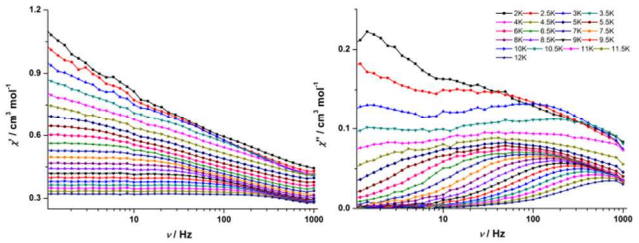

Figure 7. The frequency dependence of the out-of-phase ac susceptibility of **3** at the indicated temperature under an applied dc field of 2000 Oe.

Magnetization (*M*) data for **1c**, **2c** and **3** are collected in the 0-7 T field range below 5K. For **1c, 2c** and **3**, the magnetization *versus H/T* data at different temperatures show nonsuperposition plots, and a gradual increase of the magnetization at high fields, without a saturation even at 7 T, revealing the presence of a significant magnetic anisotropy and/or low-lying excited states. The dynamics of the magnetization for **1c**, **2c** and **3** are investigated using alternating current susceptibility measurements. A temperature dependent increase of the in-phase signal, together with the appearance of an out-of-phase signal is observed for **1c**, **2c** and **3** (Figure S16−18). It reveals the onset of slow magnetization relaxation, which is typical for SMM properties. Although the ac susceptibility as a function of the temperature does not show any peak in the out-of-phase ac susceptibility in zero dc field, it is affected by the dc field. The fast quantum tunneling of magnetization is slowed down by the applied field that the peak of the out-of-phase ac susceptibility is observed under a 2000 Oe dc filed for **2c** and **3**, as shown in Figure S20−21.

To further probe the dynamics of **1c**, **2c** and **3**, ac susceptibility measurements as a function of the frequency at different temperatures under a 2000 Oe dc field are carried out (Figure 6−7). The data plotted as Cole-Cole plots of **2c** in the temperature range of 3−9.5 K shows a relatively symmetrical shape and can be fitted to the generalized Debye model,[23] with α parameters in the range of 0.03−0.21. The relaxation time is extracted from the frequency-dependent data between 2−11 K and the Arrhenius plot obtained from these data is given in Figure 7. Above 7.5 K, the relaxation follows a thermally activated Orbach mechanism with an energy gap of 67 K and a preexponential factor τ_0 of 1.68×10^{-7} s based on the Arrhenius law [$\tau = \tau_0\exp(U_{eff}/K_BT)$]. Meanwhile, the occurrence of two distinct peaks for the out-of-phase ac signals (χ'') is evident at higher frequencies, revealing the possibility of a multiple relaxation process.[24] The Cole-Cole plots of **3** in the temperature range of 2−12 K exhibits a unique double-ridge structure as well. The anisotropic energy gaps are calculated to be 16 K (1.0×10^{-5} s) and 47 K (4.6×10^{-6} s) for the low temperature and high temperature domains, respectively. It is noted that the τ_0 values are larger than the expected values for SMM,[25] which is probably enhanced by the presence of QTM. The deviation below 7 K from Arrhenius behavior is owing to the replacement of thermally activated spin reversal by the direct process. The magnetic slow-relaxation behavior of **2c** and **3** is arisen from the presence of anisotropic Dy^{3+} ions. For **1c**, the weak signals after applying dc field show unconspicuous slow magnetic relaxation behaviour. It is possibly due to the relative close distance between Dy^{3+} ions that the weak intramolecular magnetic coupling shortcuts the thermally activated relaxations.

Conclusion

In summary, we have successfully synthesized three species of eight nma-based lanthanide complexes with acetate, nitrate, and perchlorate as the counter ions, respectively, where the ligand is in-situ generated during the reaction. Structural analysis reveals the importance of the anions in different geometries for the self-assembly and the stoichiometry. The connection of acetate groups to the Ln^{3+} ions through three coordination modes gives rise to the formation of trinuclear **1**, whilst mononuclear **2** is derived from nitrates in a single chelating mode. In the presence of uncoordinated perchlorate, the Dy is completely encapsulated by two ligands in contrast to

the cases of **1** and **2**. The complexes **1**−**3** would contribute to understand the crucial role of the anions in the assembly of the supramolecular architectures. The magnetic results of **1**−**3** highlight the possibility to tune the dynamic behavior through the adjustment on the structural environment. 2-aldehyde-8-hydroxyquinoline-based ligand would be potentially utilized for the construction of SMMs.

Acknowledgements

This work is financially supported by the National Natural Science Foundation of China (Nos. 51472076, 51302068, 21272061, 51102081 and 21102039) and the Open Project of the State Key Lab of Rare Earth Resources Utilization, CIAC.

Notes and references

[a] Key Laboratory of Functional Inorganic Material Chemistry (MOE), School of Chemistry and Materials Science, Heilongjiang University, Harbin 150080, PR China. E-mail address: jehugu@gmail.com (Chen P.); yanpf@vip.sina.com (Yan P.)

[b] State Key Laboratory of Rare Earth Resource Utilization, Changchun Institute of Applied Chemistry, Chinese Academy of Sciences, Changchun 130022, China.

† Electronic Supplementary Information (ESI) available: Crystallographic data in CIF format (CCDC 1037100-7), coordination geometries, views of the complexes and additional magnetic data. See DOI: 10.1039/b000000x/

1 (a) P. Zhang, L. Zhang, C. Wang, S. Xue and J. Tang, *J. Am. Chem. Soc*., 2014, **136**, 4484−4487; (b) S. Jiang, B. Wang, H. Sun, Z. Wang and S. Gao, *J. Am. Chem. Soc*., 2011, **133**, 4730−4733; (c) G. Christou, D. Gatteschi, D. N. Hendrickson and R. Sessoli, *MRS Bull*., 2000, **25**, 66−71.

2 (a) S. V. Eliseeva and J. C. G. Bünzli, *New J. Chem*., 2011, **35**, 1165−1176; (b) M. Norek, E. Kampert, U. Zeitler and J. A. Peters, *J. Am. Chem. Soc*., 2008, **130**, 5335−5340; (c) E. Coronado and P. Day, *Chem. Rev*., 2004, **104**, 5419−5448.

3 (a) P. E. Car, M. Perfetti, M. Mannini, A. Favre, A. Caneschi and R. Sessoli, *Chem. Commun*., 2011, **47**, 3751−3753; (b) G. Cucinotta, M. Perfetti, J. Luzon, M. Etienne, P. E. Car, A. Caneschi, G. Calvez, K. Bernot and R. Sessoli, *Angew. Chem., Int. Ed*., 2012, **51**, 1606−1610; (c) M. E. Boulon, G. Cucinotta, J. Luzon, C. Degl'Innocenti, M. Perfetti, K. Bernot, G. Calvez, A. Caneschi and R. Sessoli, *Angew. Chem., Int. Ed*., 2013, **52**, 350−354; (d) H. Wang, K. Qian, D. Qi, W. Cao, K. Wang, S. Gao and J. Jiang, *Chem. Sci*. 2014, **5**, 3214−3220.

4 (a) Y. Guo, X. Chen, S. Xue and J. Tang, *Inorg. Chem*., 2011, **50**, 9705−9713; (b) S. A. Sulway, R. A. Layfield, F. Tuna, W. Wernsdorfer and R. E. P. Winpenny, *Chem. Commun*., 2012, **48**, 1508−1510.

5 (a) J. Tang, I. Hewitt, N. T. Madhu, G. Chastanet, W. Wernsdorfer, C. E. Anson, C. Benelli, R. Sessoli and A. K. Powell, *Angew. Chem., Int. Ed*., 2006, **45**, 1729−1733; (b) I. J. Hewitt, Y. Lan, C. E. Anson, J. Luzon, R. Sessoli and A. K. Powell, *Chem. Commun*., 2009, 6765−6767; (c) F. Guo, J. Liu, J. Leng, Z. Meng, Z. Lin, M. Tong, S. Gao, L. Ungur and L. F. Chibotaru, *Chem.-Eur. J*., 2011, **17**, 2458−2466.

6 (a) P. Zhang, Y. Guo and J. Tang, *Coord. Chem. Rev*., 2013, **257**, 1728−1763; (b) D. N. Woodruff, R. E. P. Winpenny and R. A. Layfield, *Chem. Rev*., 2013, **113**, 5110−5148.

7 (a) J. D. Rinehart, M. Fang, W. J. Evans and J. R. Long, *Nat. Chem*., 2011, **3**, 538−542; (b) L. Zou, L. Zhao, P. Chen, Y. Guo, Y. Li and J. Tang, *Dalton Trans*., 2012, **41**, 2966−2971; (c) Q. Chen, Y. Meng, Y. Zhang, S. Jiang, H. Sun and S. Gao, *Chem. Commun*., 2014, **50**, 10434−10437.

8 (a) Y. Guo, G. Xu, W. Wernsdorfer, L. Ungur, Y. Guo, J. Tang, H. Zhang, L. F. Chibotaru and A. K. Powell, *J. Am. Chem. Soc*., 2011. **133**, 11948−11951; (b) R. Sessoli and A. K. Powell, *Coord. Chem. Rev*., 2009, **253**, 2328−2341; (c) S. Jiang, B. Wang, G. Su, Z. Wang and S. Gao, *Angew. Chem., Int. Ed*., 2010, **49**, 744−747; (d) N. Ishikawa, M. Sugita, T. Ishikawa, S. Koshihara and Y. Kaizu, *J. Am. Chem. Soc*., 2003, **125**, 8694−8695.

9 (a) L. Zhao, J. Wu, H. Ke and J. Tang, *Inorg. Chem*., 2014, **53**, 3519−3525; (b) W. Sun, B. Han, P. Lin, H. Li, P. Chen, Y. Tian, M. Murugesu and P. Yan, *Dalton Trans*., 2013, **42**, 13397−13403; (c) P. Yan, P. Lin, F. Habib, T. Aharen, M. Murugesu, Z. Deng, G. Li and W. Sun, *Inorg. Chem*., 2011, **50**, 7059−7065; (d) J. Long, F. Habib, P. Lin, I. Korobkov, G. Enright, L. Ungur, W. Wernsdorfer, L. F. Chibotaru and M. Murugesu, *J. Am. Chem. Soc*., 2011, **133**, 5319−5328; (e) P. Bag, A. Chakraborty, M. Rouziéres, R. Clérac, R. J. Butcher and V. Chandrasekhar, *Cryst. Growth Des*., 2014, **14**, 4583−4592.

10 (a) Y. Guo, G. Xu, P. Gamez, L. Zhao, S. Lin, R. Deng, J. Tang and H. Zhang, *J. Am. Chem. Soc*., 2010, **132**, 8538−8539; (b) P. Seth, S. Ghosh, A. Figuerola and A. Ghosh, *Dalton Trans*., 2014, **43**, 990−998.

11 (a) S. Liao, J. Shiu, S. Liu, S. Yeh, Y. Chen, C. Chen, T. Chow and C. Wu, *J. Am. Chem. Soc*., 2009, **131**, 763−777; (b) M. Albrecht, O. Osetska, J. Klankermayer, R. Fröhlich, F. Gumy and J. C. G. Bünzli, *Chem. Commun*., 2007, 1834−1836; (c) F. Rizzo, F. Meinardi, R. Tubino, R. Pagliarin, G. Dellepiane and A. Papagni, *Synth. Met*., 2009, **159**, 356−360; (d) F. Artizzu, F. Quochi, M. Saba, L. Marchiò, D. Espa, A. Serpe, A. Mura, M. L. Mercuri, G. Bongiovanni and P. Deplano, *ChemPlusChem*, 2012, **77**, 240−248; (e) N. M. Shavaleev, R. Scopelliti, F. Gumy and J. C. G. Bünzli, *Inorg. Chem*., 2008, **47**, 9055−9068; (f) S. Hossain, S. Das, A. Chakraborty, F. Lloret, J. Cano, E. Pardo and V. Chandrasekhar, *Dalton Trans*., 2014, **43**, 10164−10174.

12 M. Zhang, H. Li, P. Chen, W. Sun, L. Zhang, P. Yan, *J. Mole. Struct*. 2015. **1081**, 233−236.

13 (a) S. Konar, A. Jana, K. Das, S. Ray, S. Chatterjee and S. K. Kar, *Inorg. Chim. Acta*, 2013, **395**, 1−10; (b) F. Cui, S. Li, C. Jia, J. S. Mathieson, L. Cronin, X. Yang and B. Wu, *Inorg. Chem*., 2012, **51**, 179−187; (c) Q. Zhu, L. Yu, Y. Qin, L. Huo, M. Shao and J. Dai, *CrystEngComm*, 2011, **13**, 2521−2528; (d) J. Zhang, B. Zheng, T. Zhao, G. Li, Q. Huo and Y. Liu, *Cryst. Growth Des*., 2014, **14**. 2394−2400.

14 (a) X. Yang, M. M. Oye, R. A. Jones and S. Huang, *Chem. Commun*., 2013, **49**, 9579−9581; (b) X. Yang, D. Schipper, A. Liao, J. M. Stanley, R. A. Jones and B. J. Holliday, *Polyhedron*, 2013, **52**, 165–169; (c) X. Yang, R. A. Jones and W. Wong, *Chem. Commun*., 2008, 3266−3268.

15 (a) Z. Zheng, Y. Ou, X. Hong, L. Wei, L. Wan, W. Zhou, Q. Zhan and Y. Cai, *Inorg. Chem*. 2014, **53**, 9625−9632; (b) P. Manna, S. K. Seth, A. Bauzá, M. Mitra, S. R. Choudhury, A. Frontera and S. Mukhopadhyay, *Cryst. Growth Des*., 2014, **14**, 747−755; (c) S. Cai, M. Pan, S. Zheng, J. Tan, J. Fan and W. Zhang, *CrystEngComm*, 2012, **14**, 2308−2315; (d) G. Durá, M. C. Carrión, F. A. Jalón, A. M. Rodríguez and B. R. Manzano, *Cryst. Growth Des*., 2014, **14**, 3510−3529.

16 X. Yang, D. Schipper, R. A. Jones, L. A. Lytwak, B. J. Holliday and S. Huang, *J. Am. Chem. Soc*., 2013, 135, 8468−8471.

17 M. Hassani, W. Cai, D. C. Holley, J. P. Lineswala, B. R. Maharjan, G. R. Ebrahimian, H. Seradj, M. G. Stocksdale, F. Mohammadi, C. C. Marvin, J. M. Gerdes, H. D. Beall and M. Behforouz, *J. Med. Chem*., 2005, **48**, 7733−7749.

18 G. M. Sheldrick, SHELXL-97, Program for X-ray Crystal Structure Refinement, University of Göttingen, Göttingen, Germany, 1997.

19 A. L. Speck, *Acta Cryst*., 2015, **C71**, 9−18.

20 (a) M. U. Anwar, S. S. Tandon, L. N. Dawe, F. Habib, M. Murugesu and L. K. Thompson, *Inorg. Chem*., 2012, **51**, 1028−1034; (b) C. Liu, M. Du, E. C. Sañudo, J. Echeverria, M. Hu, Q. Zhang, L. Zhou and S. Fang, *Dalton Trans*., 2011, **40**, 9366−9369.

21 R. J. Deeth, *Inorg. Chem*., 2008, **47**, 6711−6725.

22 (a) H. L. C. Feltham and S. Brooker, *Coord. Chem. Rev*., 2014, **276**, 1−33; (b) A. Ruiz-Martínez, D. Casanova and S. Alvarez, *Chem.-Eur. J*., 2008, **14**, 1291−1303.

23 S. M. J. Aubin, Z. Sun, L. Pardi, J. Krzystek, K. Folting, L. C. Brunel, A. L. Rheingold, G. Christou and D. N. Hendrickson, *Inorg. Chem*., 1999, **38**, 5329−5340.

24 Y. Guo, G. Xu, P. Gamez, L. Zhao, S. Lin, R. Deng, J. Tang and H. Zhang, *J. Am. Chem. Soc*., 2010, **132**, 8538−8539.

25 (a) Y. Gao, G. Xu, L. Zhao, J. Tang and Z. Liu, *Inorg. Chem*., 2009, **48**, 11495−11497; (b) F. Tuna, C. A. Smith, M. Bodensteiner, L. Ungur, L. F. Chibotaru, E. J. L. McInnes, R. E. P. Winpenny, D. Collison and R. A. Layfield, *Angew. Chem., Int. Ed*., 2012, **51**, 6976−6980; (c) F. Pointillart, S. Klementieva, V. Kuropatov, Y. L. Gal, S. Golhen, O. Cador, V. Cherkasov and L. Ouahab, *Chem. Commun*., 2012, **48**, 714−716..

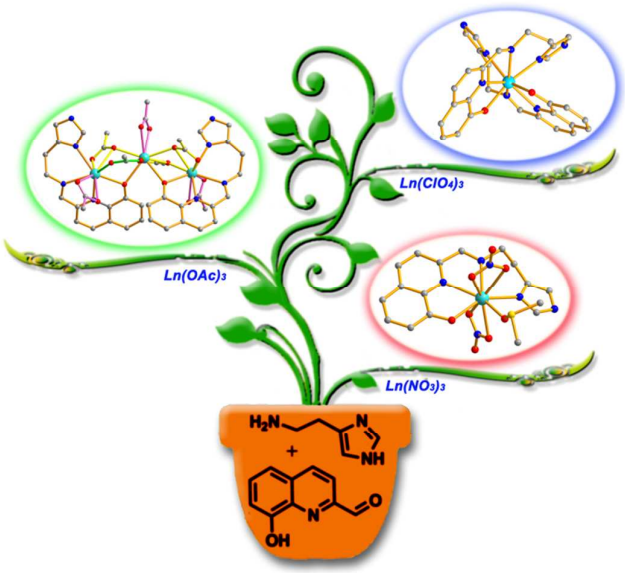

The *in-situ* reaction of 2-aldehyde-8-hydroxyquinoline, histamine and $LnX_3 \cdot 6H_2O$ ($X^- = OAc^-$, NO_3^- and ClO_4^-) affords three distinct species of eight lanthanide complexes.